PNAS

Supporting Information for

Epitranscriptomic cytidine methylation of the Hepatitis B viral RNA is essential for viral reverse transcription & particle production

Pei-Yi (Alma) Su[a], Chih-Hsu Chang[a], Shin-Chwen Bruce Yen[a, b], Hsiu-Yi Wu[a], Wan-Ju Tung[a], Yu-Pei Hu[c], Yen-Yu Ian Chen[c], Miao-Hsia Lin[d], Chiaho Shih[e], Pei-Jer Chen[f], Kevin Tsai[a, 1]

[a] Institute of Biomedical Sciences (IBMS), Academia Sinica, Taipei, Taiwan
[b] Taiwan International Graduate Program (TIGP), National Yang-Ming Chiao-Tung University and Academia Sinica, Taipei, Taiwan
[c] IBMS Summer Undergraduate Internship Program, Academia Sinica, Taipei, Taiwan
[d] Graduate Institute and Department of Microbiology, National Taiwan University College of Medicine, Taipei, Taiwan
[e] Graduate Institute of Cell Biology, College of Life Sciences, China Medical University, Taichung, Taiwan
[f] National Taiwan University Center for Genomic Medicine, National Taiwan University; Graduate Institute of Clinical Medicine, National Taiwan University College of Medicine; Department of Internal Medicine, National Taiwan University Hospital, Taipei, Taiwan.
[1] Lead Contact

Correspondence: Email: kevtsai@ibms.sinica.edu.tw. Tel: +886-2-2652-3934

This PDF file includes:

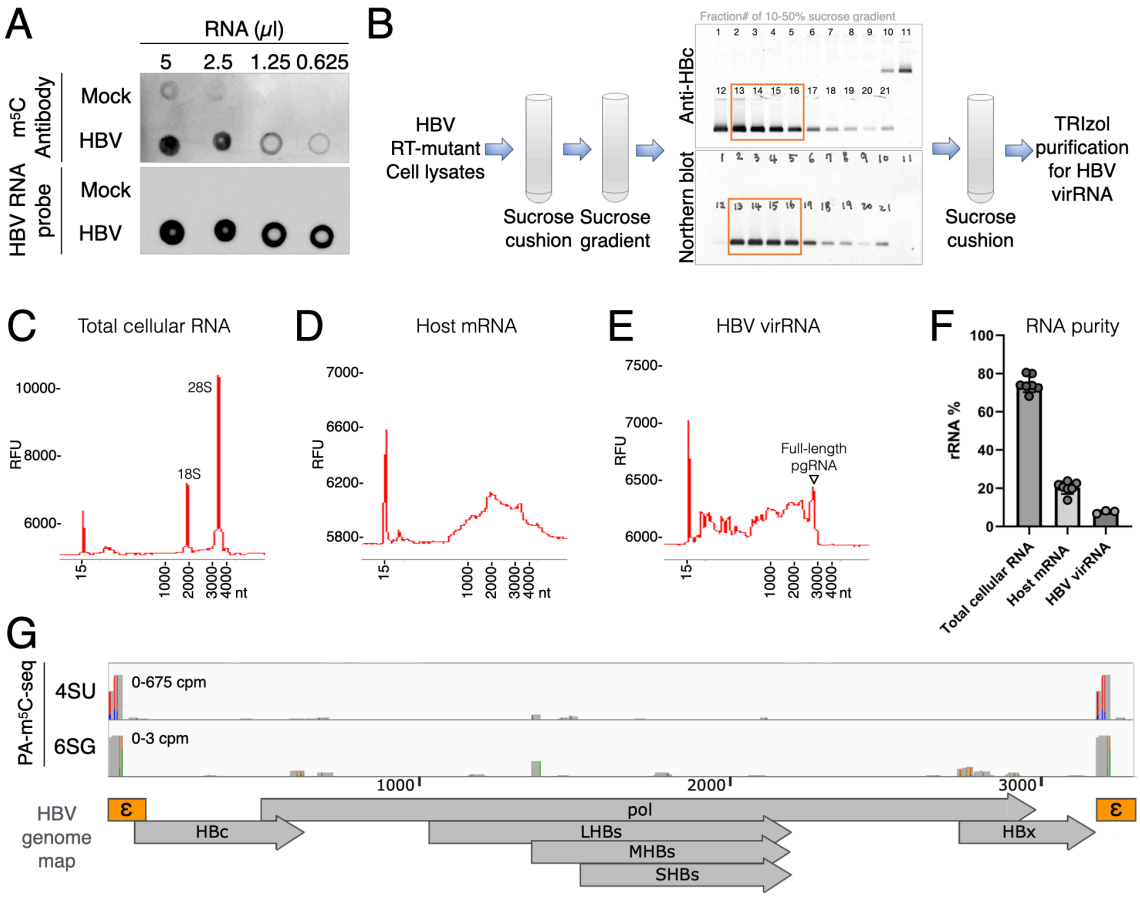

Fig. S1. Detection of m^{5}C on HBV RNA via orthogonal methods. (A) Dot blot assay of m^{5}C on RNA extracted from supernatants of HuH-7 cells with HBV or without HBV (mock, top panel), then counter stained for HBV RNA by Northern blot in the lower panel. **(B)** Flow chart of the purification of HBV RNA from RT-mutant replicon -transfected HuH-7 cells for UPLC-MS/MS modification quantification. Following sucrose gradient separation, RNA was extracted from viral capsid HBc-containing fractions (red-boxed lanes). **(C-F)** Capillary RNA electrophoresis (Fragment Analyzer) traces of total cellular RNA **(C)**, the poly(A) purified and ribo-depleted HuH-7 mRNA **(D)**, and HBV viral RNA extracted as in panel B **(E)**. Purified RNA shown in panels D and E were used for UPLC-MS/MS modification analysis shown in Figs. 1A-1B and Table 1. **(F)** Area under curve quantifications of 18S and 28S rRNA proportions in total cellular RNA, or purified host mRNA, and HBV virion RNA, from repeats of panels C-E. **(G)** PA-m^{5}C-seq done on HBV transcripts by 4SU-mediated crosslinking (top lane, copied from Fig. 1C) shown compared to PA-m^{5}C-seq done with 6SG-mediated crosslinking (bottom lane).

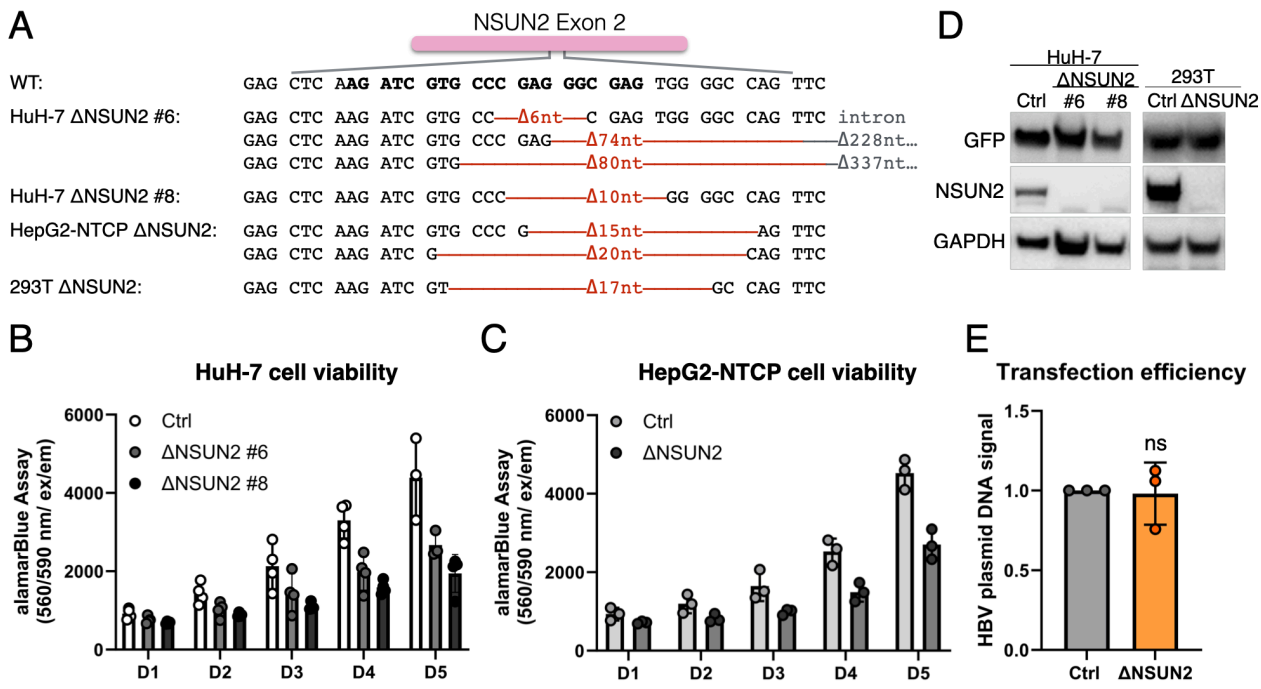

Figure S2. Characterization of CRISPR-generated NSUN2-depleted cell lines. (A) Sequencing analysis of the CRISPR-edit site on NSUN2 exon 2 in ΔNSUN2 HuH-7, HepG2-NTCP and 293T cells. **(B-C)** Viability of ΔNSUN2 HuH-7 and HepG2-NTCP cells compared to control (Ctrl), measured by the resazurin-based alamarBlue cell metabolic activity assay. **(D)** Western blot analysis of transfection efficiency in Ctrl versus ΔNSUN2 HuH-7 and 293T cells, as tested with a transfected GFP expression vector. **(E)** Efficiency of HBV replicon transfection efficiency in Ctrl & ΔNSUN2 HuH-7 cells assayed via DNA qPCR 24hrs post-transfection. ns = not significant.

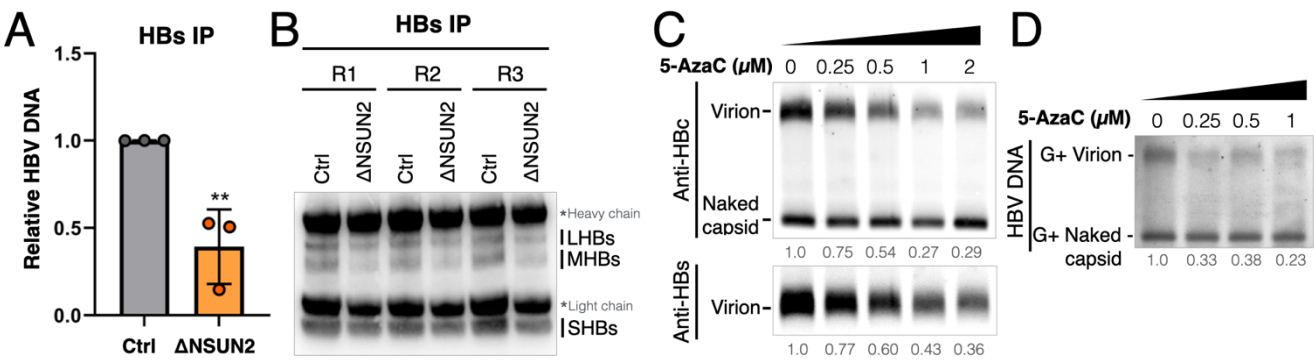

Figure S3. NSUN2 depletion and pharmacological disruption of NSUN2 function leads to loss of virion DNA production. (A-B) Secreted HBV virions from Ctrl & ΔNSUN2 HuH-7 cells were immunoprecipitated using anti-HBs antibody **(B)** and the enclosed HBV DNA quantified via qPCR, normalized to HBs protein levels, shown relative to Ctrl set as 1 **(A)**. **(C-D)** HBV-transfected HuH-7 cells were treated with 5-AzaC as in Fig. 2I, and analyzed for secreted virion HBc and HBs by Western blot **(C)**, as well as secreted viral DNA by Southern blot **(C)**.

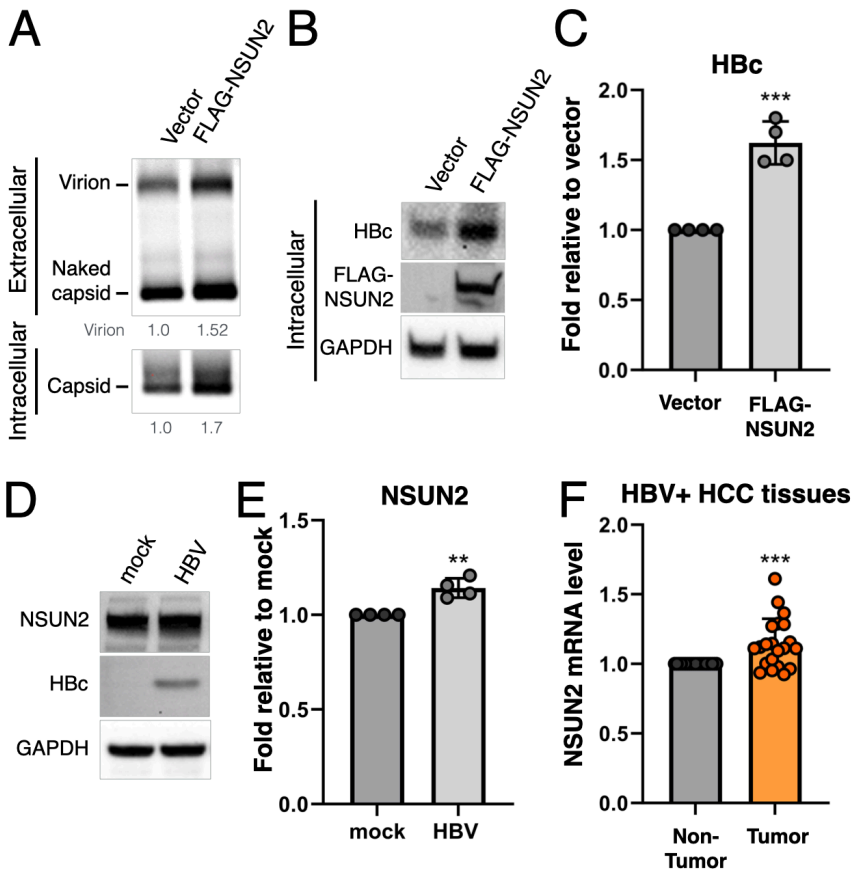

Figure S4. NSUN2 overexpression enhances HBV replication while HBV led to minimal host NSUN2 expression increase. (A) To test if NSUN2-overexpression enhances HBV replication, HuH-7 cells were transfected with empty vector or a FLAG-NSUN2 expression plasmid, the extracellular virions and intracellular capsids assayed via native gel capsid protein Western blot. **(B)** Intracellular HBc and FLAG-NSUN2 proteins were assayed by Western blot for HBc and FLAG-tagged protein levels **(C)** Repeats of panel B quantified. **(D)** Endogenous NSUN2 expression assessed via Western blotting in HuH-7 cells transfected with empty vector or an HBV replicon. **(E)** Repeats of panel D quantified. **(F)** NSUN2 mRNA levels in HBV-infected HCC patient tissues compared with surrounding non-tumor tissue (19 tumor/non-tumor patient sample pairs, RNA-seq data from GEO: GSE94660) Error bars = SD; $**p < 0.01$, $***p < 0.001$.

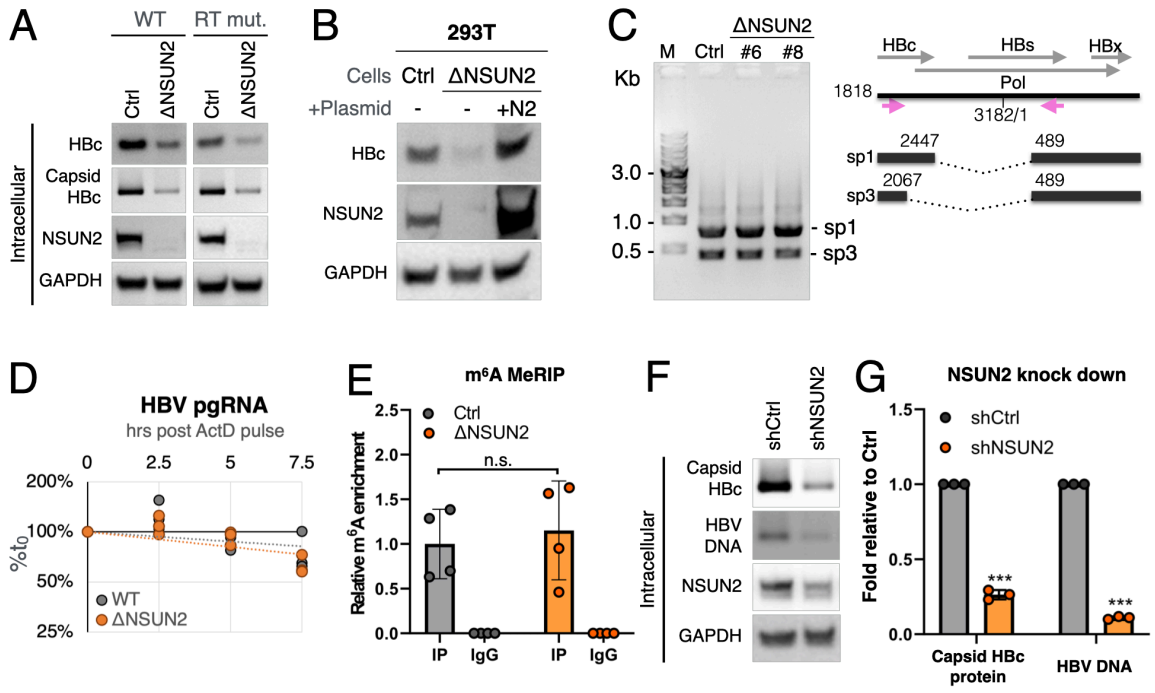

Figure S5. NSUN2 enhances HBV HBc and DNA production, with no evidence of regulating viral RNA stability, splicing or m^{6}A methylation. (A) Intracellular HBc and capsid-particle-forming HBc protein levels measured by Western blot in WT/RT-mut. HBV-transfected Ctrl and ΔNSUN2 HuH-7 cells, representative of repeats summarized in Figs. 4C & 4F. **(B)** HBc protein expression assayed in Cas9 control (Ctrl) or NSUN2 knockout (ΔNSUN2) 293T cells transcomplemented with an NSUN2 expression vector (+N2) or empty vector (-), transfected with a wildtype HBV replicon. **(C)** HBV major RNA splice variants sp1 and sp3 measured by RT-PCR in HBV-transfected Ctrl and ΔNSUN2 HuH-7 cells. Diagram of splice variants to the left, with red arrows depicting the PCR primers used. **(D)** pgRNA stability assessed by RT-qPCR following Actinomycin D (ActD) pulse-chase in HBV-transfected Ctrl and ΔNSUN2 HuH-7 cells. **(E)** HBV RNA m^{6}A levels quantified via m^{6}A RNA immunoprecipitation (MeRIP) in HBV-transfected Ctrl and ΔNSUN2 HuH-7 cells, n=4. **(F)** Intracellular capsid HBc protein and HBV DNA were measured by native agarose gel Western blot and Southern blot, respectively, in HBV-transfected shRNA-mediated NSUN2 knockdown HuH-7 cells (shNSUN2). **(G)** Band intensities of three repeats of panel F. Error bars = SD; ***p < 0.001; 'n.s.' = not significant.

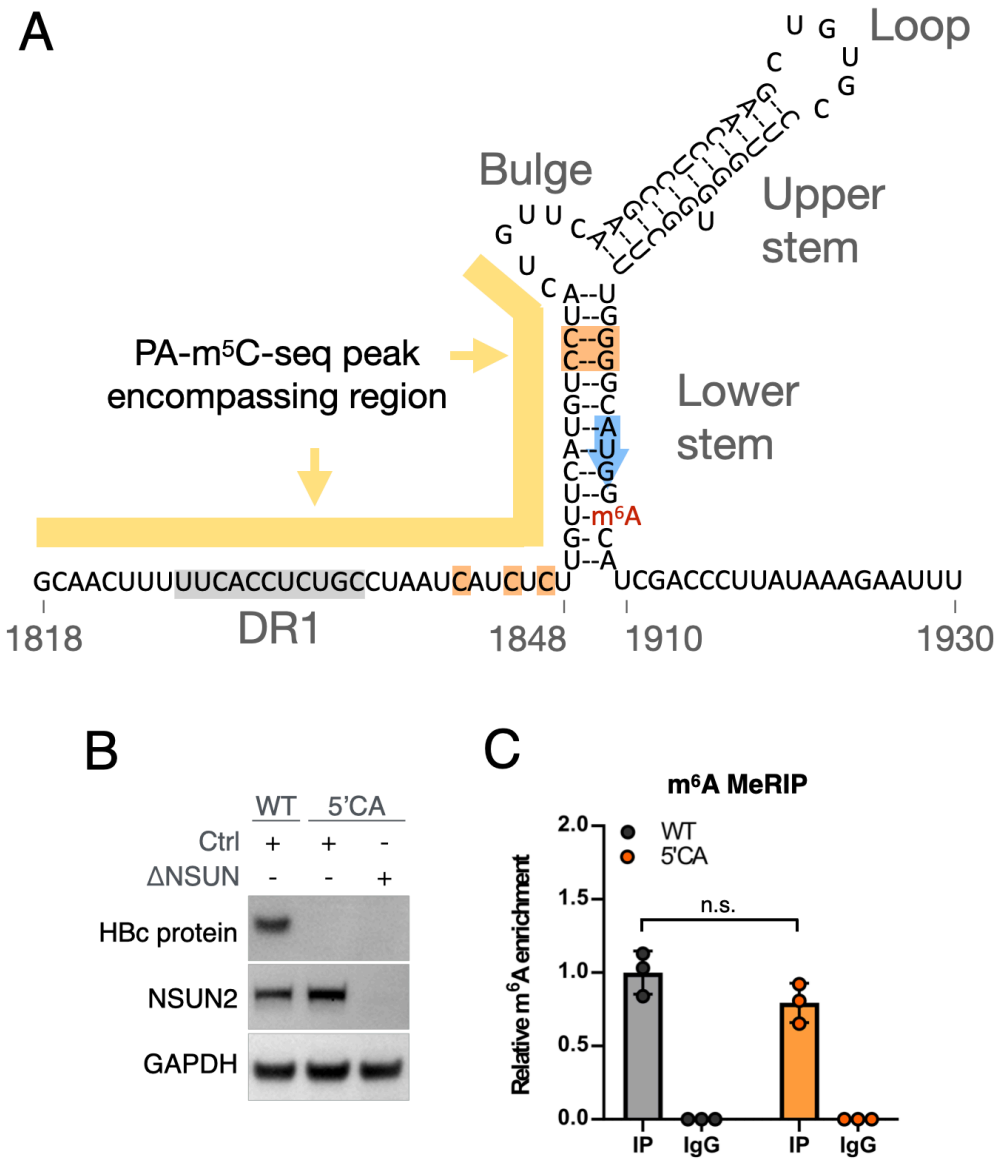

Figure S6. Mutational removal of putative m^{5}C sites leads to diminished HBV replication without affecting viral RNA m^{6}A levels. (A) Diagram of mapped m^{5}C peak and mutation sites on the epsilon hairpin structure. The known hairpin structure of epsilon (1), with the mapped m^{5}C/NSUN2-bound region shown with a yellow bar, the direct repeat 1 (DR1) element in gray, the HBc start codon in the blue arrow, and mutated cytidines highlighted in orange. C1853 in the left lower stem was kept intact, as mutating this C would necessitate mutating the G in the HBc start codon to preserve the hairpin structure. Shown nucleotide numbers correspond to the ayw strain genome (GenBank J02203), 1818nt here corresponds to 1nt and 3183nt in our dual epsilon maps shown in Fig. 1. A1907 depicted as m^{6}A in red to show the previously reported methylation site (2). **(B)** Western blot assay of HBc protein expression from WT or 5'CA mutant HBV replicon transfected WT or ΔNSUN2 HuH-7 cells. **(C)** m^{6}A levels on WT or 5'CA mutant HBV RNA quantified via MeRIP in HuH-7 cells transfected with the corresponding replicon, n=3.

Table S1. List of nucleotide standards used for UPLC-MS/MS peak identification and standard curve setup.

Source	Cat. #	Nucleotide abbreviation	Nucleotide
Sigma/Supelco (nucleotide mix)	47310-U	C	Cytidine
		G	Guanosine
		I	Inosine
		m1A	1-Methyladenosine
		m5C	5-Methylcytidine
		Cm	2′-O-Methylcytidine
		m3C	3-Methylcytidine methosulfate
		m7G	7-Methylguanosine
		m5U	5-Methyluridine
		ψ	β-Pseudouridine
		2sC	2-Thiocytidine dihydrate
		U	Uridine
Acros/Thermo	164040050	A	Adenosine
Toronto Research Chemicals	M276150	Am	2'-O-Methyl Adenosine
Toronto Research Chemicals	M275895	m6A	N6-Methyladenosine
MedChemExpress	HY-W013260-100MG	Gm	2'-O-Methylguanosine
Toronto Research Chemicals	N633048	ac4C	N4-Acetylcytidine
MedChemExpress	HY-W011824-250MG	Um	2'-O-Methyluridine

Table S2. List of primers and oligos used in this study

Oligo name	Sequence		Reference
Gene Cloning			
NSUN2-F	5'-ATAGGTACCATGGGGCGGCGGTCGCGGGG	For cloning NSUN2 into p3XFlag-CMV14	This study
NSUN2-R	5'-ATATCTAGACCGGGGTGGATGGACCCCCG	For cloning NSUN2 into p3XFlag-CMV14	This study
NSUN4-F	5'-ATAGGTACCATGGCTGCGCTGACACTGAG	For cloning NSUN4 into p3XFlag-CMV14	This study
NSUN4-R	5'-ATAGGATCCTGTCAGCCTACGCATTTTGC	For cloning NSUN4 into p3XFlag-CMV14	This study
NSUN5-F	5'-ATAGGTACCATGGGGCTGTATGCTGCAGC	For cloning NSUN5 into p3XFlag-CMV14	This study
NSUN5-R	5'-ATATCTAGATGTGCAAGGCGGTGTGCAAG	For cloning NSUN5 into p3XFlag-CMV14	This study
NSUN6-F	5'-ATAGGTACCATGTCTATTTTCCCTAAGAT	For cloning NSUN6 into p3XFlag-CMV14	This study
NSUN6-R	5'-ATAGGATCCTGTGCTTTTGCATTTTACAA	For cloning NSUN6 into p3XFlag-CMV14	This study
NSUN2 depletion			
sgNSUN2-F	5'-CACCGAGATCGTGCCCGAGGGCGAG	NSUN2-targeting SpCas9 sgRNA for insert into LentiCRISPR2	GeCKOv2 Library #HGLibA_32780
sgNSUN2-R	5'-AAACCTCGCCCTCGGGCACGATCTC	NSUN2-targeting SpCas9 sgRNA for insert into LentiCRISPR2	GeCKOv2 Library #HGLibA_32780
NSUN2-genotyping-F	5'-aaaggatcccCTTAGAGCTGTTCGCTGTT	PCR ~1kb surounding the expected cut site of guide #HGLibA_32780 on the human genome	This study
NSUN2-genotyping-R	5'-aaaaagcttTCCTAAGCATATCCTACCGTTAAGT	PCR ~1kb surounding the expected cut site of guide #HGLibA_32780 on the human genome	This study
NSUN2-crRes1-F	5'-gagctcaaAatTgtCccTgaAggGgaAtggggccag	Site-directed mutagenesis primer for generating NSUN2 expression vector resistant to guide #HGLibA_32780	This study
NSUN2-crRes1-R	5'-ctggccccaTtcCccTtcAggGacAatTttgagctc	Site-directed mutagenesis primer for generating NSUN2 expression vector resistant to guide #HGLibA_32780	This study
NSUN2 Knockdown	Target Sequence		
shCtrl (Scramble)	CCTAAGGTTAAGTCGCCCTCG	Knockdown control	ASN0000000003

shNSUN2	GCGTGTTAGAAATCACTTGTT	NSUN2 knockdown	TRCN0000297585
qPCR			
HBV-qPCR-F	5'-GAGTGTGGATTCGCACTCC	HBV pgRNA RT-qPCR/ HBV DNA qPCR	PMID: 27783675
HBV-qPCR-R	5'-GAGGCGAGGGAGTTCTTCT	HBV pgRNA RT-qPCR/ HBV DNA qPCR	PMID: 27783675
HBV-qPCR 5'-Epsilon-F	5'-GCATGGACATCGACCCTTATA	HBV epsilon-specific qPCR primer for m6A MeRIP	This study
HBV-qPCR 5'-Epsilon-R	5'-AGAATTGCTTGCCTGAGTGC	HBV epsilon-specific qPCR primer for m6A MeRIP	This study
Site-Directed Mutagenesis			
HBV-Mutagenesis-CG-1	5'-TTTTCACCTCTGCCTAATGATGTGTTGTTCATGTGGTACTGTTCAAGCCTCCAA	Site-Directed Mutagenesis for Mutant 5'CG, 3'CG	This study
HBV-Mutagenesis-CG-2	5'-GTGCCTTGGGTGGCTTTGCCGCATGGACATCGACCCTTATAAA	Site-Directed Mutagenesis for Mutant 5'CG, 3'CG	This study
HBV-Mutagenesis-CA-1	5'-TTTTCACCTCTGCCTAATAATATATTGTTCATGTAATACTGTTCAAGCCTCCAA	Site-Directed Mutagenesis for Mutant 5'CA, 3'CA	This study
HBV-Mutagenesis-CA-2	5'-GTGCCTTGGGTGGCTTTGTTGCATGGACATCGACCCTTATAAA	Site-Directed Mutagenesis for Mutant 5'CA, 3'CA	This study
Splice RNA			
pgRNA-SpliceRNA-F	5'-AGCCTCCAAGCTGTGCCTTGGGTG	PCR primer for HBV splice RNA detection	PMID: 30800119
pgRNA-SpliceRNA-R	5'-AACCACTGAACAAATGGCACTAGTAAACTGAGC	PCR primer for HBV splice RNA detection	PMID: 30800119

SI Methods and Materials

shRNA-mediated generation of NSUN2 knockdown HuH-7 cells

293T cells were transfected with lentiviral packaging plasmids (dR8.74 and pMD2.G) and pLKO-shRNA plasmids containing either NSUN2-targeting or scrambled shRNAs. Lentivirus supernatants was collected on days 3 and 5. The supernatant was then concentrated using a 10% PEG solution (10% PEG-8000, 0.3M NaCl). The concentrated lentivirus was used to infect HuH-7 cells in a 10 cm dish for 24 hours, followed by Puromycin (4 μg/ml) selection for 5 days to establish a polyclonal stable knockdown cell line. pLKO-shRNAs were purchased from the Academia Sinica RNAi core (TRC2 scrambled control #ASN0000000003; shNSUN2 #TRCN0000297585).

Generation of Gene Knock Out 293T Cells

ΔNSUN2 293T cell lines were generated through CRISPR/Cas9 genome editing as mentioned in the main text methods section for ΔNSUN2 HuH-7 cells.

Expression plasmid construction

FLAG-tagged NSUN2, NSUN4, NSUN5 or NSUN6 plasmids were cloned by PCR from HuH-7 cDNA and ligated into p3XFLAG-CMV-14 (a kind gift from Joanne Jeou-Yuan Chen).

Dot blot

5 million Huh7 cells in 10cm plates were transfected with empty vector (mock) or the HBV 1.1mer replicon expressing a RT-defective mutant pol Y63D (3, 4). 5 days post transfection, 40mls of mock and HBV Y63D+ supernatant were harvested and concentrated using 10% PEG-8000 and incubated at 4°C overnight. Following centrifugation, the pellets were resuspended in 200 μL of TNE (10 mM Tris–HCl (pH 7.4), 150 mM NaCl, and 1 mM EDTA) solution. Subsequently, viral RNAs were purified using the High Pure Viral Nucleic Acid Kit (Roche). The purified RNAs were then applied to an N+ Nylon membrane (Invitrogen) and cross-linked twice with 150mJ/cm2 of UV light 254nm (Stratalinker 2400, Stratagene). After blocking with 5% non-fat milk, the membrane was hybridized with m5C antibody (#C15200081, Diagenode), counterstained with an anti-mouse IgG-HRP antibody and visualized using ECL.

RNA modification profiling by UPLC-MS/MS

Highly purified RNA digested to single nucleosides were analyzed using UPLC-MS/MS at the Academia Sinica Agricultural Biotechnology Research Center (ABRC) metabolomics core, following published procedures (5). Briefly, the Ultra-Performance Liquid Chromatography system (ACQUITY UPLC, Waters, Millford, MA) was coupled to the Waters Xevo TQ-XS triple quadrupole mass spectrometer (Waters, Milford, USA). The sample was separated using an ACQUITY Premier HSS T3 column (1.8μm particle size, 2.1 × 100mm, Waters), at a flow rate of 0.2 mL/min and column temperature of 40℃. Characteristic MS transitions were monitored using multiple reaction monitoring (MRM) mode. Data acquisition and processing were performed using MassLynx v4.2 and TargetLynx software (Waters Corp.).

Pseudouridine was specifically quantified with aliquots of the filtered nucleosides ran on an Agilent 1290 Infinity II ultra-high performance liquid chromatography (uHPLC) equipped with a HSS T3 column (Waters 2.1×100 mm, 1.8 μm), with a flow rate of 0.2 mL/min at 25°C. The MS/MS spectra of analytes were acquired using Agilent 6495C triple quadruple LC/MS with positive electrospray ionization (ESI+) mode. The peak areas of each analyte were generated using Agilent MassHunter QQQ Quantitative Analysis software.

Quantitation of all modifications was based on a spiked-in 13C9, 15N3 radioisotope cytidine as an internal standard (13C9H1315N3O5, Cambridge Isotope # CNLM-3807-5), with nucleotide standards (Table S1) run at three magnitudes of dilutions to set up standard curves.

Total RNA-seq

To elucidate the expression levels of each transcript in the samples used for m5C & m6A mapping, RNA-seq was done on an aliquot of the poly(A) purified mRNA used for the m5C/m6A pulldowns as input controls. 1.5μg of poly(A) selected mRNA was incubated at 94°C for 70secs in 50μl fragmentation buffer (0.01M ZnCl2 with 0.01M Tris pH7.0), the reaction then immediately

stopped by the addition of EDTA to a final concentration of 0.02M on ice. The fragmented RNA was purified using Zymo RNA clean & concentrator 5 columns, dephosphorylated with 2U of Shrimp Alkaline Phosphatase (rSAP, NEB) with a 37°C 20min incubation and subsequent 65°C 5mins heat inactivation, and re-phosphorylated with T4 Polynucleotide Kinase (NEB) at 37°C for 20mins with 0.33mM ATP, 3.3mM MgCl2, 10U T4 PNK, and 5mM DTT. The resulting end-repaired RNA fragments were then purified again with Zymo RNA clean & concentrator 5 columns.

PA-m^{5}C-seq with 6-thioguanosine-dependent crosslinking

For the 2nd lane in Fig. S1H, PA-m5C-seq was done as described in the main methods, but with 100mM of 6-thioguanosine (6SG, MedChemExpress HY-119499) in place of 4SU. 6SG crosslinking results in A>G conversions instead, thus sequencing reads with this conversion signature were computationally picked out for downstream analysis, with all other analysis steps the same as standard PA-m5C-seq.

PAR-CLIP

Five 15cm plates, each containing 7 million HuH-7 cells, were co-transfected with either FLAG-GFP or FLAG-NSUN2 along with the HBV 1.1mer replicon. 2 days post transfection, the virus-containing cells were supplemented with 100μM 4SU and harvested 18hrs later following on-plate crosslinking with 2500×100 μJ/cm2 of 365 nm UV. The cells were lysed in RIPA buffer and subject to PAR-CLIP pulldown with a FLAG antibody, as previously described (6, 7).

Illumina Sequencing & Bioinformatics Analysis

All RNA-seq, PA-m6A/m5C-seq, and PAR-CLIP RNA samples were subject to library preparation using the NEBNext Multiplex Small RNA Library Prep Set for Illumina (NEB #E7330), and sequenced with an Illumina HiSeq2500 sequencer at the Academia Sinica Biodiversity Research Center (BRCAS) High Throughput Sequencing Core, or an Illumina NextSeq500 sequencer at the Academia Sinica Institute of Molecular Biology (IMB) Genomics Core. Sequencing data was done as before (8, 9). Briefly, adaptor sequences were removed using FASTX-toolkit v0.0.14, while also removing any reads <15nt and/or with fastq quality score <33. Reads which past the above quality control were aligned to the human genome (hg19) using Bowtie v1.2.3 (10), and the human non-aligning reads subsequently aligned (allowing no more than 1 mismatch) to a reordered HBV subtype ayw genome with one copy of epsilon on each end. Our reordered HBV genome is GenBank #J02203.1 with nucleotides 1818-3182(end) forming the first half, and subsequently joined with nucleotides 1-1937 of J02203.1, thus 1818-1937nt of J02203.1 (which covers epsilon) is duplicated on both ends of our reordered HBV genome to better represent the pgRNA. For PA-m5C/m6A-seq and PAR-CLIP reads, alignments with the characteristic T>C conversions resulting from UV-crosslinked 4SU were selected with all other alignments discarded. Alignment files were finally converted to bam files using SAMtools (11) and visualized via Integrative Genomics Viewer (IGV) (12). The viral gene annotations shown in figures accompanying sequencing coverage maps were generated by downloading the GenBank full annotation file from NCBI nucleotide J02203.1, doing the epsilon reordering as described above, and visualized using Snapgene viewer (Dotmatics).

Aza-IP

HuH-7 cells seeded the previous day at 2.5x106 per dish were co-transfected with 1.5 μg HBV RT-deficient mutant Y63D replicon and equal amounts of FLAG-tagged NSUN2, NSUN4, NSUN5 or NSUN6 expression vectors. Transfected cells were treated with 5μM of 5-AzaC 24hrs prior to harvest, and replaced 12hrs later to account for drug decay (13). Cell lysates harvested at 72 hours post-transfection were lysed in RIPA buffer [50mM Tris-HCl pH 7.5, 150mM NaCl, 1% SDS, 0.5% DOC, 1% NP-40, 2mM TCEP pH 7, pH7.0, 1x protease inhibitor (#P8340, Sigma-Aldrich)]. Immunoprecipitation was done using mouse IgG (#I5381, Sigma-Aldrich) or anti-FLAG antibody (#F1804, Sigma-Aldrich) pre-incubated 1hr with Dynabeads Protein G (#10004D, Invitrogen), followed by six washes in NET-2 buffer (50mM Tris-HCl pH 7.5, 150mM NaCl, 0.05% NP-40, 2mM TCEP pH 7, 1x protease inhibitor) and two washes in High-Salt wash buffer (50mM HEPES-KOH pH 7.5, 500mM KCl, 0.05% NP-40, 2mM TCEP pH 7, 1x protease inhibitor).

Pulldown efficiencies were assessed by Western blots of aliquots of each sample, and the remaining samples subject to Trizol RNA extraction, reverse transcription and qPCR to quantify the pulled down RNA.

ELISA

The levels of HBs and HBe proteins were assessed using an ELISA assay (General Biologicals Corporation), following manufacturer procedures.

Cell proliferation and cytotoxicity assay

The HuH-7 cell proliferation and cytotoxicity assay were examined with or without the addition of 5-AzaC (Sigma) compounds at concentrations ranging from 0 to 5 μM. To measure cell proliferation, Cell Counting Kit-8 (CCK-8, Dojindo Molecular Technologies, Inc.) were used. To evaluate cytotoxicity, Cytotoxicity LDH Assay Kit-WST (Dojindo Molecular Technologies, Inc.) were used.

Quantification of HBV virion DNA by HBs-IP qPCR

Done as previously described (14). Briefly, HBV virions were immunoprecipitated from the viral supernatant using a rabbit anti-HBs antibody (Novus) and Dynabeads™ Protein G beads (Invitrogen) at 4°C with overnight rotation. Viral DNA was extracted using the High Pure Viral Nucleic Acid Kit (Roche). HBV virion DNA was quantified by qPCR.

RNA stability assay

Done as previously described (9). Briefly, HuH7 and ΔNSUN2 HuH-7 cells were transfected with HBV and then treated with actinomycin D (5μg/ml) at 2 days post-transfection. Cells were harvested at 0, 2.5, 5, and 7.5 hours. HBV RNA was quantified by qRT-PCR.

m^{6}A meRIP-qPCR

10μg of HBV-transfected HuH-7 cell total RNA was treated with DNase I (NEB) and fragmented to ~500bps by incubating in 10 mM ZnCl2, 10 mM Tris-HCl pH 7.0 at 94°C for 45secs. The fragmented RNA was co-incubated with 1 μg of rabbit anti-m6A antibody (Abcam #ab151230) and Dynabeads™ Protein G beads (Invitrogen) in MeRIP binding buffer (10 mM Tris-HCl, 150 mM NaCl, 0.1% NP-40, pH 7.4) at 4°C with overnight rotation. The immunoprecipitated beads were washed with MeRIP wash buffer (10 mM Tris-HCl, 1 M NaCl, 0.1% NP-40, pH 7.4), and the pulled-down RNA purified using TRIzol. The input RNA (10% of IP RNA) and IP RNA were quantified by RT-qPCR.

Characterization of CRISPR-generated NSUN2-depleted cell lines

Initially, loss of NSUN2 protein from HuH-7, HepG2-NTCP, and 293T cells was validated by Western blot. For NSUN2 knockout genotyping, the genomic DNA from NSUN2 depleted cells were purified by Quick-DNA Miniprep Plus Kit (Zymo) and then NSUN2 exon2 genomes were amplified by PCR, followed by TA cloning into pGEM T-vector (Promega) for Sanger sequencing. The metabolic activity of NSUN2-depleted cells were assessed using the alamarBlue assay (Thermo Fisher Scientific), with excitation at 569 nm and emission at 590 nm for measuring relative fluorescence units. To evaluate transfection efficiency, cells were transfected with a GFP expression vector, and GFP expression was detected via Western blotting. Additionally, DNA transfection efficiency was also quantified through HBV plasmid DNA qPCR analysis conducted 24 hours post-transfection.

HBV RNA splicing detection

1 μg of total RNA extracted from HBV-transfected HuH-7 control and ΔNSUN2 cells were reverse transcribed to cDNA using random hexamers and SuperScript™ III Reverse Transcriptase (Thermo Fisher Scientific). Subsequently, the HBV splicing RNA was detected via semiquantitative PCR as previously described (15). The resulting PCR products was visualized through agarose gel electrophoresis.

NSUN2 trans-complementation

HuH-7 control and ΔNSUN2 cells were transfected with either an empty vector or a pLEX-NSUN2 expression plasmid (with silent mutations rendering it resistant to our NSUN2 CRISPR guide). One day post transfection, wildtype HBV-replicon was transfected into the same cells and maintained for 3 days. The rescue effect of NSUN2 on HBc protein expression was assessed via Western blotting. Similarly, the NSUN2 transcomplementation study was performed in 293T cells. HBV replicon and either pLEX-NSUN2 (CRISPR resistant) or vector plasmids were co-transfected into both Cas9 control (Ctrl) and NSUN2 knockout (ΔNSUN2) 293T cells. After 3 days post-transfection, HBc protein expression was evaluated via Western blot analysis.

SI References

1. J. E. Tavis, S. Perri, D. Ganem, Hepadnavirus reverse transcription initiates within the stem-loop of the RNA packaging signal and employs a novel strand transfer. *J Virol* **68**, 3536-3543 (1994).
2. H. Imam *et al.*, N6-methyladenosine modification of hepatitis B virus RNA differentially regulates the viral life cycle. *Proc Natl Acad Sci U S A* **115**, 8829-8834 (2018).
3. M. Nassal, The arginine-rich domain of the hepatitis B virus core protein is required for pregenome encapsidation and productive viral positive-strand DNA synthesis but not for virus assembly. *J Virol* **66**, 4107-4116 (1992).
4. R. E. Lanford, L. Notvall, H. Lee, B. Beames, Transcomplementation of nucleotide priming and reverse transcription between independently expressed TP and RT domains of the hepatitis B virus reverse transcriptase. *J Virol* **71**, 2996-3004 (1997).
5. M. Basanta-Sanchez, S. Temple, S. A. Ansari, A. D'Amico, P. F. Agris, Attomole quantification and global profile of RNA modifications: Epitranscriptome of human neural stem cells. *Nucleic Acids Res* **44**, e26 (2016).
6. M. Hafner *et al.*, Transcriptome-wide identification of RNA-binding protein and microRNA target sites by PAR-CLIP. *Cell* **141**, 129-141 (2010).
7. K. Tsai *et al.*, Epitranscriptomic addition of m(6)A regulates HIV-1 RNA stability and alternative splicing. *Genes Dev* **35**, 992-1004 (2021).
8. D. G. Courtney *et al.*, Epitranscriptomic Addition of m(5)C to HIV-1 Transcripts Regulates Viral Gene Expression. *Cell Host Microbe* **26**, 217-227 e216 (2019).
9. K. Tsai *et al.*, Acetylation of Cytidine Residues Boosts HIV-1 Gene Expression by Increasing Viral RNA Stability. *Cell Host Microbe* **28**, 306-312 e306 (2020).
10. B. Langmead, C. Trapnell, M. Pop, S. L. Salzberg, Ultrafast and memory-efficient alignment of short DNA sequences to the human genome. *Genome Biol* **10**, R25 (2009).
11. H. Li *et al.*, The Sequence Alignment/Map format and SAMtools. *Bioinformatics* **25**, 2078-2079 (2009).
12. J. T. Robinson *et al.*, Integrative genomics viewer. *Nat Biotechnol* **29**, 24-26 (2011).
13. V. Khoddami, B. R. Cairns, Identification of direct targets and modified bases of RNA cytosine methyltransferases. *Nat Biotechnol* **31**, 458-464 (2013).
14. C. H. Chang, S. F. Chou, C. Shih, A nuanced role of the small loop of hepatitis B virus small envelope protein in virion morphogenesis and secretion. *J Biomed Sci* **28**, 82 (2021).
15. N. Ito, K. Nakashima, S. Sun, M. Ito, T. Suzuki, Cell Type Diversity in Hepatitis B Virus RNA Splicing and Its Regulation. *Front Microbiol* **10**, 207 (2019).